

# Atmospheric Reentry of a Hydrazine Tank

Robert L. Kelley, William C. Rochelle,  
ESCG  
Houston, TX

## Introduction

The purpose of this white paper is to describe the methods used to predict the survivability of a titanium tank loaded with frozen hydrazine reentering the Earth's atmosphere. The paper begins by describing the details of the problem, followed by the methods used to gather required data for a reentry simulation. This paper also presents results created during the analysis. The focus of the paper is a discussion of the heat transfer methods used; therefore, only a brief discussion regarding calculations of net heat rates to the body, trajectory calculations, and aerodynamic calculations are presented.

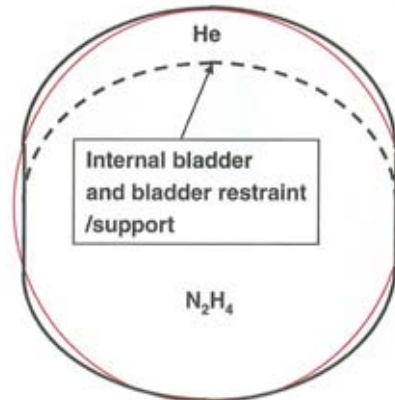
## Problem

The initial presentation of the problem was that of a tank containing frozen hydrazine ( $N_2H_4$ ) contained within a vehicle reentering the atmosphere due to natural decay from a nearly circular orbit. The tank is essentially spherical with a diameter of 1.0414 meters (41 inches) and a wall thickness of 0.00356 meters (0.14 inches). In addition, the tank contained 453.59 kg (1000 lbs) of frozen  $N_2H_4$ .

## Propulsion Tank



- Very close to spherical
  - (see red line below)
- 41" diameter
- 0.140" thick Ti wall
- 106 lbs dry
- 400 psig operating pressure
- 1000 lbs  $N_2H_4$



### Gathering Required Data for Modeling

The properties of N<sub>2</sub>H<sub>4</sub> required for the analysis were the specific heat capacity (C<sub>p</sub>), thermal conductivity, density, emissivity, heat of fusion, oxide heat of formation, and melting temperature. These values are summarized in Table 1 below. The specific heat capacity for liquid was found to be 3084.1 J/kg-K (Ref. 1). Using a relationship between the specific heat capacity of ice to that of water (approximately 0.506), C<sub>p</sub> for liquid N<sub>2</sub>H<sub>4</sub> was multiplied by that value to get a value of 1559.45 J/kg-K. The thermal conductivity was found to be 1.57 W/m-K. The density of N<sub>2</sub>H<sub>4</sub> was found to be 1025.3 kg/m<sup>3</sup> at 0° C which is below the freezing point of 2° C (Ref. 1). An emissivity value of 0.5 was arbitrarily assigned. The heat of fusion for N<sub>2</sub>H<sub>4</sub> was found to be 395024.9 J/kg (Ref 1.). The oxide heat of formation was set to 0, as this value only applies to metals. Finally, the melting temperature was found to be 275 K.

Property	Value
specific heat capacity, C <sub>p</sub> (J/kgK)	1559.45
thermal conductivity, k (W/mK)	2.4
density, rho (kg/m <sup>3</sup> )	1025.3
emissivity,	0.5
heat of fusion (J/kg)	395024.97
oxide heat of formation (J/kg-O <sub>2</sub> )	0
melting temperature, T <sub>m</sub> (K)	275

Table 1 - Summary of N<sub>2</sub>H<sub>4</sub> Properties

In addition to the properties of the N<sub>2</sub>H<sub>4</sub>, the same properties were required for Ti, which in this case was assumed to be Titanium (6 Al-4 V). For this material C<sub>p</sub>, thermal conductivity, and emissivity are all temperature dependant, and plots of these values can be seen below in Figures 1-3, respectively. The remaining values are summarized in Table 2 below (Ref. 2).

Property	Value
specific heat capacity, C <sub>p</sub> (J/kgK)	Figure 1
thermal conductivity, k (W/mK)	Figure 2
density, rho (kg/m <sup>3</sup> )	4437
emissivity,	Figure 3
heat of fusion (J/kg)	393559
oxide heat of formation (J/kg-O <sub>2</sub> )	32481250
melting temperature, T <sub>m</sub> (K)	1943

Table 2 - Summary of Ti (6 Al-4 V) Properties

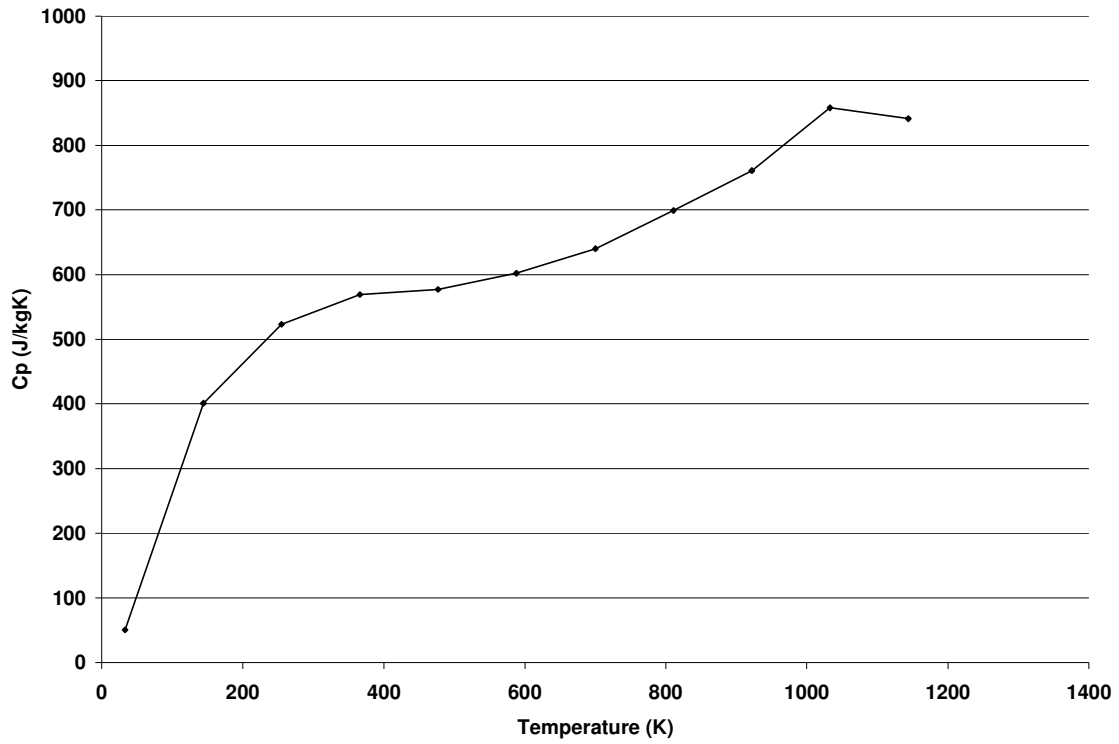


Figure 1 – Specific Heat Capacity (J/kgK) of Ti (6 Al-4 V) vs. Temperature (K)

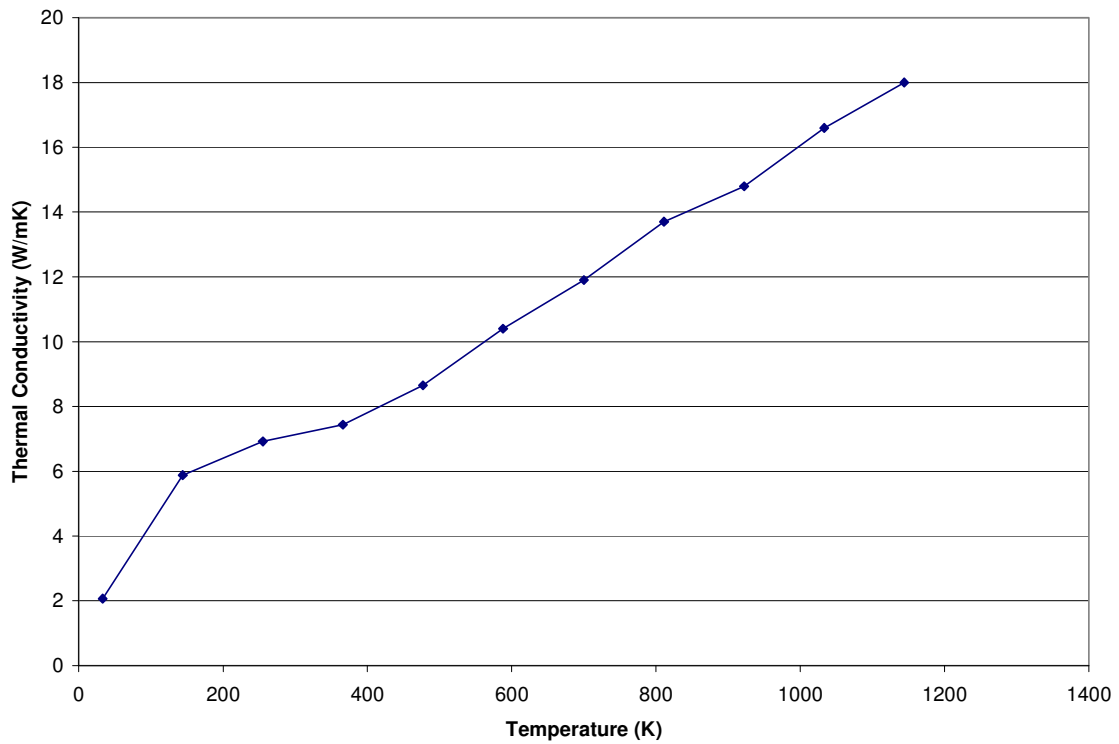
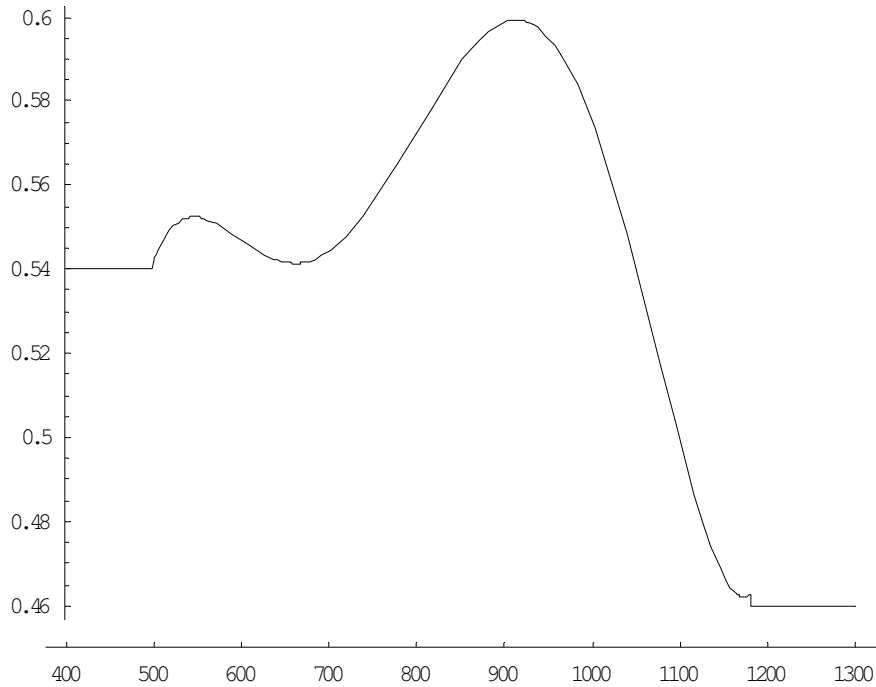


Figure 2 – Thermal Conductivity (W/mK) of Ti (6 Al-4 V) vs. Temperature (K)



**Figure 3 – Emissivity of Ti (6 Al-4 V) vs. Temperature (K)**

**(Note: For temperatures below 400 K emissivity is constant 0.54 and for temperatures above 1300 K emissivity is a constant 0.46)**

Modeling the heat transfer through and into a partially filled tank undergoing reentry into the atmosphere presents several challenges. The volume of the tank is approximately  $0.579 \text{ m}^3$  of which the  $\text{N}_2\text{H}_4$  occupies  $0.442 \text{ m}^3$ , assuming a density of  $\text{N}_2\text{H}_4$  at  $0^\circ \text{C}$  of  $1025.3 \text{ kg/m}^3$  and the mass of 453.6 kg. The remaining volume contains a pressurant and an internal bladder and bladder restraint/support. The  $\text{N}_2\text{H}_4$ , therefore, is in contact with only a portion of the interior wall of the tank. Initially, the principal heat transfer modes would be via conduction where the  $\text{N}_2\text{H}_4$  is in contact with the tank wall and via radiation elsewhere.

Based upon experience, the vehicle containing the tank will probably break-up due to aerodynamic forces at an altitude of approximately 78 km. At this time the tank should separate from the vehicle intact under spin, and the pressure inlet and the  $\text{N}_2\text{H}_4$  outlet lines should be severed. These lines normally are made of lower melting temperature materials and, again from experience, are assumed to burn off completely during reentry, resulting in the release of the pressurant and the exposure of the frozen  $\text{N}_2\text{H}_4$  to a small outlet opening. The effect of the openings on the heat transfer process are assumed to be negligible.

If the heat transfer process is sufficient to permit initially melting of the  $\text{N}_2\text{H}_4$  in immediate contact with the inner wall of the tank, this liquid  $\text{N}_2\text{H}_4$  will be susceptible to expulsion from the tank, hindering potential convection processes. If sufficient  $\text{N}_2\text{H}_4$  is melted, the remaining frozen  $\text{N}_2\text{H}_4$  would no longer be firmly in contact with the inner wall of the tank and would be susceptible to internal movement and fracture from forces associated with the spinning, decelerating tank.

Two bounding heat transfer modeling techniques were considered. The first envisioned a solid ball of frozen N<sub>2</sub>H<sub>4</sub> in the center of the tank with a vacuum (following depressurization of the tank at the time of vehicle break-up) between it and the tank inner wall. In such a case, the principal subsequent heat transfer mode into the N<sub>2</sub>H<sub>4</sub> would be via radiation. Alternatively, the N<sub>2</sub>H<sub>4</sub> could be envisioned as a uniform shell, i.e., material layer, affixed to the complete inner wall of the tank with a dead space in the center. This internal layer of N<sub>2</sub>H<sub>4</sub> would have a thickness of 0.197 m. Both cases were analyzed. The second case (material layer), relying on more efficient conduction heat transfer processes, would represent a better opportunity for melting of the N<sub>2</sub>H<sub>4</sub> and is described below.

The initial temperature of the tank and the N<sub>2</sub>H<sub>4</sub> was dictated to be 214 K for this study, although the actual temperature would very likely be higher. The initial relative velocity at an altitude of 78 km was set to 7.58 km/sec, and the initial flight path angle was chosen as -0.2°, a standard value for a spacecraft reentering from a nearly circular orbit.

### **Trajectory**

This analysis utilized a 3-Degree-of-Freedom (3-DOF) trajectory propagated by integrating relative equations of motion for the time rate of change of altitude, relative velocity, relative flight path angle, and longitude. To solve these trajectory equations a 4<sup>th</sup> order Runge-Kutta numerical scheme is used. For orbital decay the relative velocity and flight path angle are input, which for this case were 7.58 km/sec and -0.2°, respectively. Since this is an uncontrolled reentry an initial longitude of 0° is assigned.

### **Atmosphere**

The atmosphere model used for this analysis was the U. S. Standard Atmosphere 1976 model (Ref. 3). This is a steady-state (year-round) model of the Earth's atmosphere at latitude 45°N during moderate solar activity.

### **Aerodynamics**

The drag coefficient is used to compute the ballistic coefficient contained in the trajectory equations for time rate of change velocity. The present analysis was for that of a sphere, which was considered to be spinning. For a spinning sphere there are two constant values of the drag coefficient; one for the free-molecular regime, and one for the continuum regime, which are 2.00 and 0.92, respectively. For the transitional regime a modified Lockheed bridging function based on reference 4 is used as:

$$C_{D_{tran}} = C_{D_{cont}} + \left( C_{D_{fm}} - C_{D_{cont}} \right) \left\{ \sin \left[ \pi \left( 0.5 + 0.25 \log_{10} Kn \right) \right] \right\}^3 \quad (1)$$

where the continuum and free molecular values are as above, and Kn is the Knudson number.

### **Aerothermodynamics**

The methods used to calculate convective heating rates in this analysis are based on the object geometry (in this case a sphere), Stanton No., and Knudson No. within free-molecular flow, continuum flow, or transitional flow in which a bridging function is used.

For a sphere the stagnation point cold wall heating rate in continuum flow is obtained from the Detra, Kemp and Riddell method of reference 5. For free molecular flow the following equation is used:

$$q_{st_{fm},cw} = \frac{\alpha_T \rho_\infty V_\infty^3}{2} \quad (2)$$

where  $\alpha_T$  = thermal accommodation coefficient = 0.9 .

This equation applies for values of Knudsen numbers greater than 10.0. If the thermal accommodation coefficient of equation 2 were set equal to 1, the stagnation heating rate would give the maximum heat rate due to kinetic energy in the flow. For transitional flow ( $0.01 < Kn < 10$ ), the variation of Stanton No. versus Knudson number based on Cropp (Ref. 6) is obtained from a table look up and the stagnation point heat rate is defined by:

$$\dot{q}_{st_{trans}} = St(0.5\rho_\infty V_\infty^3) \quad (3)$$

where St is the Stanton number,  $\rho_\infty$  is the free stream density, and  $V_\infty$  is the free stream velocity.

The cold wall heating rate is multiplied by a factor that accounts for the average heating over the surface due to spinning of the sphere (0.275 for continuum, and 0.25 for free molecular). This cold wall heating rate is then converted to a hot wall value based on the following enthalpy ratio:

$$q_{hw} = q_{cw} \left( \frac{h_{st} - Cp_{air} T_w}{h_{st} - Cp_{air} T_{cw}} \right) \quad (4)$$

where stagnation enthalpy,  $h_{st}$ , is computed as

$$h_{st} = \frac{V_\infty^2}{2} + Cp_{air} T_\infty \quad (5)$$

where  $V_\infty$  is the free-stream velocity and the temperature of the cold wall,  $T_{cw}$ , is set to 214 K in this analysis. The specific heat of air,  $Cp_{air}$ , is taken as a function of wall temperature,  $T_w$

$$\begin{aligned} Cp_{air} &= 1373 \frac{\text{J}}{\text{kg} - \text{K}}, & T_w &\geq 2000\text{K} \\ Cp_{air} &= 959.9 + 0.15377T_w + 2.636 \times 10^{-5} T_w^2, & 300\text{K} &\leq T_w \leq 2000\text{K} \\ Cp_{air} &= 1004.7 \frac{\text{J}}{\text{kg} - \text{K}}, & T_w &\leq 300\text{K} \end{aligned} \quad (6)$$

The net heating rate to a reentering object is computed as the sum of the hot wall heating rate, the oxidation heating rate, and the gas cap radiative heating rate (negligible for orbital or suborbital entry), minus the reradiative heating rate. The oxidation heating rate is based on the heat of oxidation of the material and an oxidation efficiency (usually assumed to be the mean value of 0.5). The reradiation heat rate is based on the time-varying wall temperature raised to the fourth power and the surface emissivity.

### Heat Transfer

For a spinning sphere this analysis assumed a 1D heat conduction model, meaning that heat was assumed to be conducted only in the radial direction. With the N2H4 being treated as a material layer of the sphere, a standard finite difference method was used. Utilizing a Forward Time Central Space finite difference solution for a hollow sphere, the temperature response can be determined. The differential equation for this 1D thermal math model (TMM) is written in spherical coordinates as:

$$\rho C_p \frac{\partial T}{\partial t} = \frac{1}{r^2} \frac{\partial}{\partial r} \left( k r^2 \frac{\partial T}{\partial r} \right) \quad (7)$$

At each interior node  $j$  in a 1D TMM, the temperature is computed using the following finite difference relationships for the absorbed heat  $Q$ :

$$Q_{in} = G(T_{j+1} - T_j)\Delta t \quad (8)$$

$$Q_{out} = G(T_j - T_{j-1})\Delta t \quad (9)$$

$$T_i = T_{i-1} + \frac{Q_{in} - Q_{out}}{mC_p} \quad (10)$$

where the subscripts  $i, j$  refer to the current value, and node ( $j=1$  being the interior node), respectively, and  $G$  is the radial conductor defined as:

$$G = \frac{4\pi k}{\frac{1}{r_1} - \frac{1}{r_2}}; \quad (11)$$

where  $k$  is the thermal conductivity defined in the material properties and  $m$  is the mass of the node.

At the surface

$$T_{wall} = \frac{q_{net} A_s}{G} + T_{old} \quad (12)$$

$$Q_{in} = G(T_{wall} - T_{old})\Delta t \quad (13)$$

$$q_{net} = q_{hw} + q_{ox} - q_{rr} \quad (14)$$

where  $q_{net}$  is the net heating rate to the outer wall,  $q_{hw}$  is the hot wall convective heating rate,  $q_{ox}$  is the oxidation (or chemical) heating rate,  $q_{rr}$  is reradiative heating rate, and  $A_s$  is the surface area. Since several parameters are dependant on the surface temperature, an iteration is performed to converge to the surface temperature at each time step (Ref. 2).

In order for the outer Ti skin to lose nodes or ablate, the absorbed heat must be greater than the heat of ablation, or

$$Q_{in} > H_{ablat} = m[h_f + Cp(T_{melt} - T_i)] \quad (15)$$

where  $h_f$  = the heat of fusion for the material, and  $m$  is the mass of the layer.

## Results

Under the initial conditions and modeling techniques described above, it was found that the N2H4 located inside of the Ti tank does not reach its melting temperature, only reaching a maximum temperature of 255.6 K. During this time the Ti tank does reach 1943 K, its melting temperature, and four of its five nodes do ablate, but the heat absorbed into the Ti is insufficient for it to ablate the final node based on Eq. (15). Using the mass of 453.6 kg, and the assumed heat capacity of 1559.45 J/kg-K, the N2H4 would have needed to absorb 43.15 MJ of energy (heat of ablation) to reach 275 K from the start temperature of 214 K. It only absorbed 29.34 MJ, or about 68% of that.

Figure 4 below shows the net heating rate to the tank, as well as each of the heating rate components used to calculate  $q_{net}$ , all with respect to time. It can be seen from the plot that the maximum net heating rate occurs early in the trajectory (at about 10 seconds), reaching about 22 W/cm<sup>2</sup>. Figure 5 shows the net heating again, as well as the total absorbed heat into the body and the total heat absorbed into the N2H4 layer, again with respect to time. As addressed above, the maximum heat absorbed into the N2H4 is about 29.34 MJ. Figures 6 and 7 both plot the temperature of the N2H4 as a function of time, with figure 6 including the tank surface temperature and figure 7 showing an expanded scale of the N2H4 temperature.



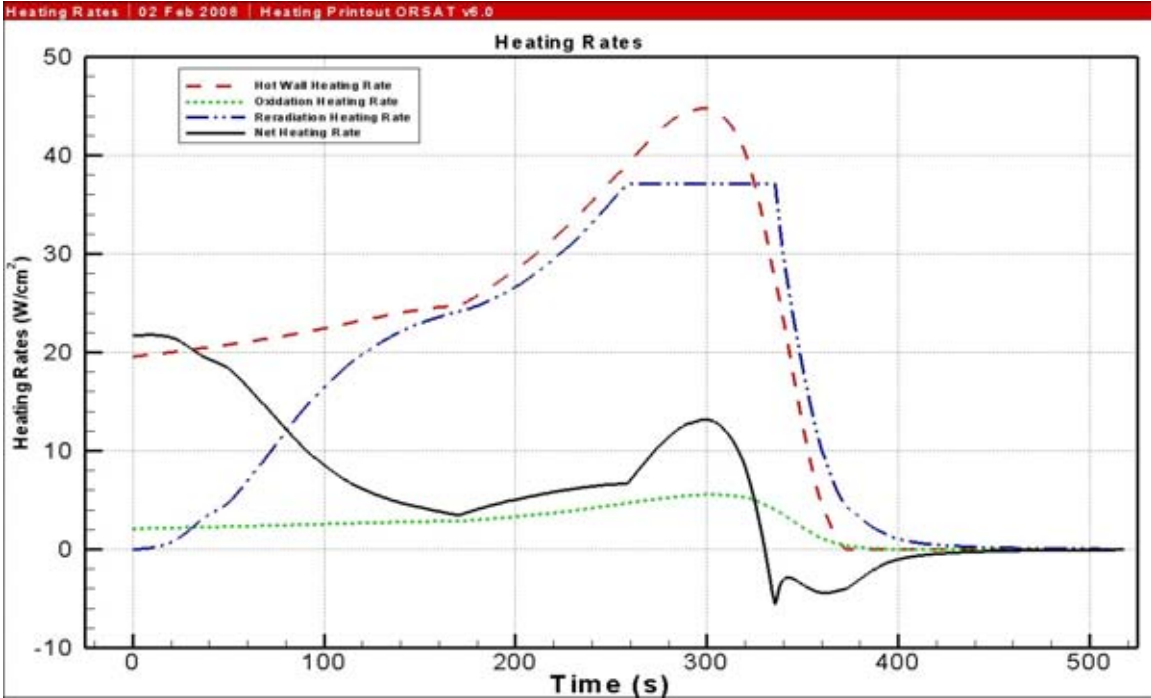


Figure 4 – Component Heat Rates (W/cm<sup>2</sup>) vs. Time (s)

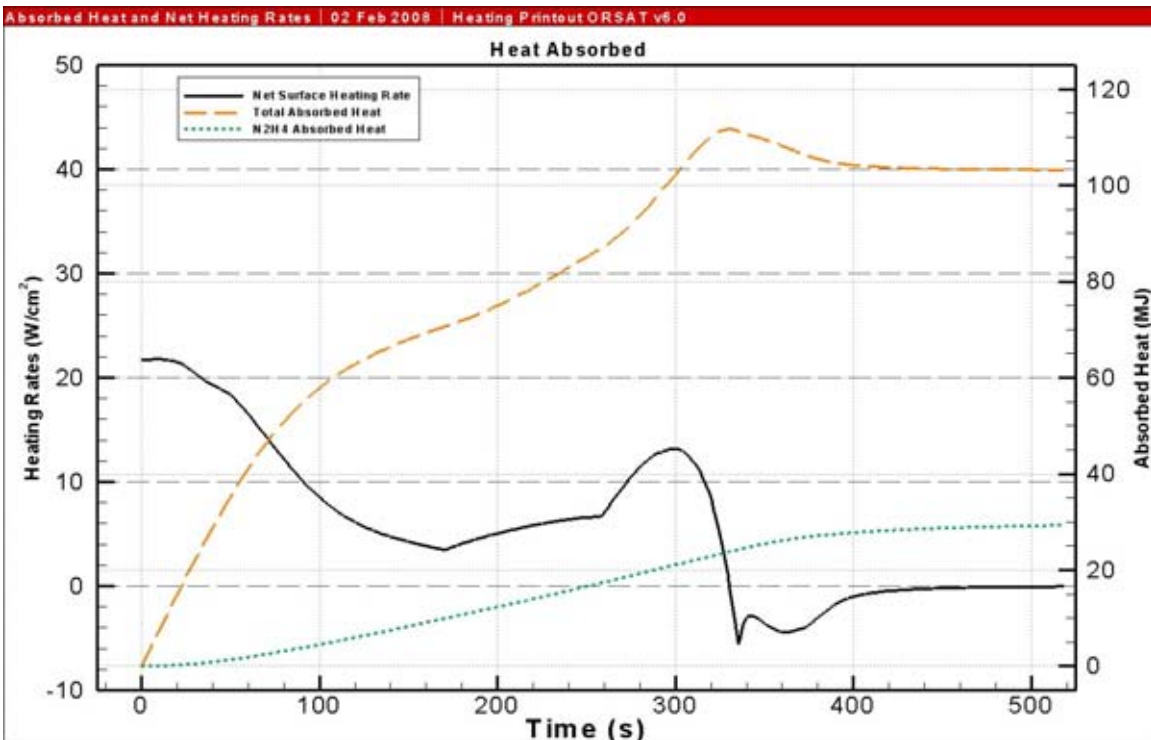


Figure 5 – Heat Absorbed (MJ) and Net Heating Rate (W/cm<sup>2</sup>) vs. Time (s)

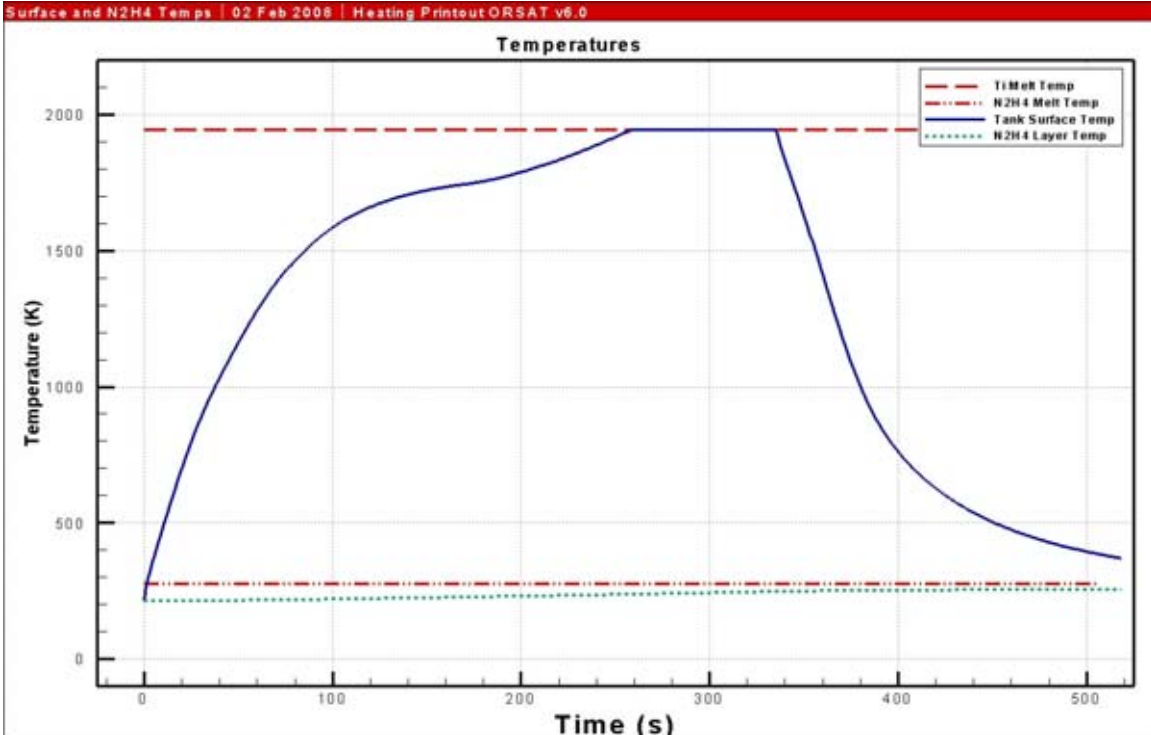


Figure 6 – Ti Surface and N2H4 Layer Temperatures (K) vs. Time (s)

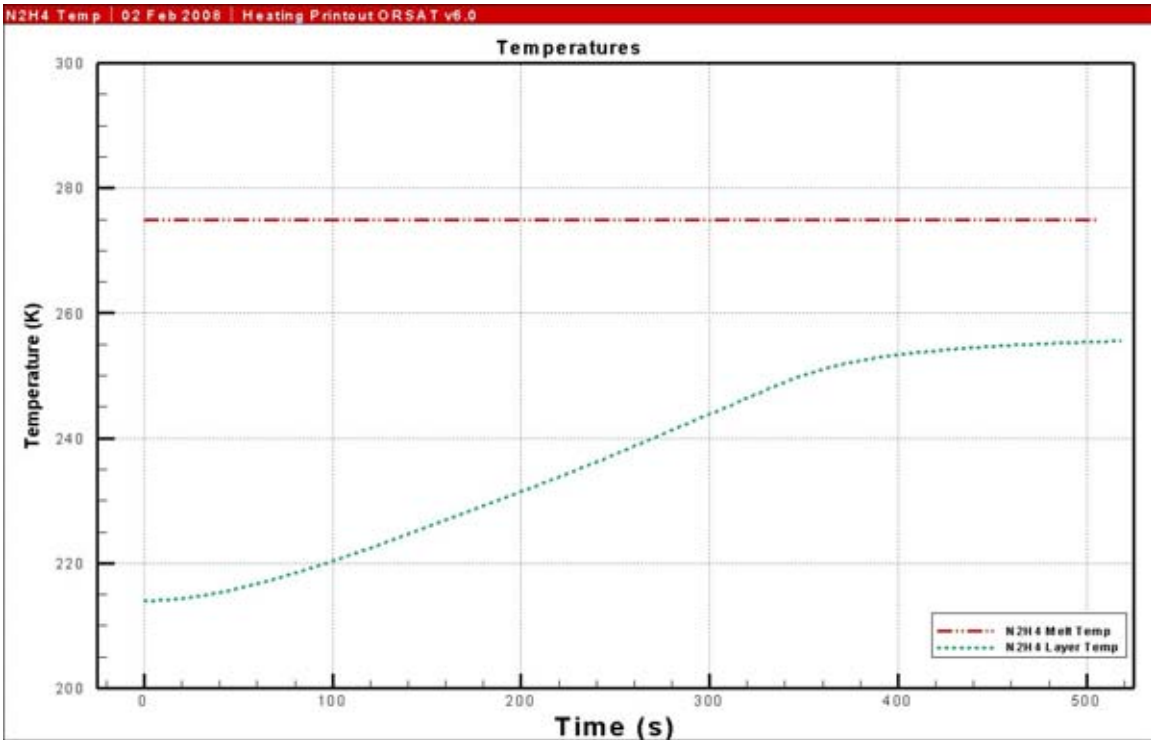


Figure 7 – N2H4 Layer Temperature (K) vs. Time (s)

## Conclusions

As applied in this analysis, the assumptions for the materials and the heating rate methods do not predict that the N<sub>2</sub>H<sub>4</sub> would melt during reentry due to orbital decay. In addition to these assumptions, there are also simplifications made for this analysis which may impact the results. The treatment of the frozen N<sub>2</sub>H<sub>4</sub> has presented itself as a unique challenge.

Of the N<sub>2</sub>H<sub>4</sub> material values used in the present analysis, the specific heat capacity remains to be the one value based on the properties of other materials. In addition, most of the material data used here is set to constant values, while typically material properties show some sort of temperature dependence. Any improvements to the material model of N<sub>2</sub>H<sub>4</sub> will impact the results produced.

The simplification in this model which could have the largest impact is also difficult to address. It is extremely likely that the N<sub>2</sub>H<sub>4</sub> in contact with the Ti wall will melt away in layers. As modeled in this analysis, the N<sub>2</sub>H<sub>4</sub> is treated as a single layer, meaning that enough heat must be absorbed to raise the temperature of the entire mass of N<sub>2</sub>H<sub>4</sub>, and then enough heat must be absorbed to melt the entire mass. Current limitations in the process being used prevent the option of splitting the N<sub>2</sub>H<sub>4</sub> into multiple layers, thereby impacting the fidelity of the model in this scenario. As noted previously, any melted N<sub>2</sub>H<sub>4</sub> might be expected to be expelled from the tank through the open propellant outlet or even through the pressurants inlet, if the bladder is ruptured. In such a case, the principal heat transfer mode would reset to conduction.

## References

1. Handbook, Hydrazine AeroJet Redmond Operations.
2. Dobarco-Otero, J.; Smith, R. N.; Bledsoe, K. J.; De Laune R. M.: JSC-62861, User's Guide for Object Reentry Survival Analysis Tool (ORSAT) – Version 6.0, Vols. I, January 2006
3. *U. S. Standard Atmosphere, 1976*, Government Printing Office, Washington, DC, 1976.
4. Wojciechowski, C. J.; and Penny, M. M.: LMSC-HREC D162867-I, Development of High Altitude Plume Impingement Analysis for Calculating Heating Rates, Forces, and Moments, Volume I – Final Report. Lockheed Missiles & Science Company, 1971.
5. Detra, R. W., Kemp, N. H., and Riddell, F. R., “Addendum to Heat Transfer to Satellite Vehicles Reentering the Atmosphere,” *Jet Propulsion*, Vol. 27, No. 12, December 1957, pp. 1256-57.
6. Cropp, L. O.: SC-RR-65-187, Analytical Methods used in Predicting the Re-Entry Ablation of Spherical and Cylindrical Bodies. Sandia Corporation, Sept. 1965.